JOURNAL OF SPACECRAFT AND ROCKETS
Vol. 35, No. 3, May–June 1998

# Launch Vehicle Self-Sustained Oscillation from Aeroelastic Coupling Part 2: Analysis

K. W. Dotson,* R. L. Baker,† and R. J. Bywater‡
*The Aerospace Corporation, Los Angeles, California 90009-2957*

**Aeroelastic theory developed in a companion paper is applied to the analysis of a launch vehicle mission, and the corresponding loads are compared with those for other transonic events. Limit cycle amplitudes are computed for several payload fairing lengths using both the present theory and the classical approach for analysis of launch vehicle aeroelastic coupling. The present theory explicitly identifies a generalized time lag as the critical parameter for aeroelastic coupling. The amplitude of the self-sustained oscillation can be significantly smaller than that predicted by the so-called stability criterion in the classical theory, depending on the value of this parameter. The single mode representation for launch vehicle aeroelastic analysis is assessed through transient analysis of the fully coupled system. It is shown that higher-order Fourier components of the oscillating flow forces can excite system modes other than the bending mode, which was expected to dominate the coupling. Data exhibiting oscillating flow states during a flight of the Titan IV launch vehicle are presented.**

## Nomenclature

| | |
|---|---|
| $D$ | = diameter of payload fairing (PLF), in. |
| $f$ | = frequency, Hz |
| $\{L\}$ | = vector of launch vehicle loads, lbf and lbf-in. |
| [LTM] | = transformation matrix for displacement-based loads; e.g., lbf/in. and lbf-in./in. |
| $M$ | = Mach number, dimensionless |
| $n$ | = index in Fourier series, dimensionless |
| $q$ | = generalized translation for a single system mode, in. |
| $T$ | = period, s |
| $t$ | = time, s |
| $U$ | = velocity of external flow, in./s |
| $x$ | = distance aft of the PLF cone–cylinder junction, in. |
| $z$ | = generalized translation normalized with respect to its static value, dimensionless |
| $\alpha$ | = rigid-body angle of attack in the pitch plane, deg |
| $\Delta t$ | = generalized time lag, the sum of the dynamic and aerodynamic time lags, s |
| $\Delta t_a$ | = aerodynamic time lag for flow state change, s |
| $\Delta t_d$ | = dynamic time lag for initiation of flow state change, s |
| $\zeta$ | = structural damping (as a ratio to the critical value) for a single system mode, dimensionless |
| $\theta$ | = rotation, rad or deg |
| $\{\phi\}$ | = system mode vector, dimensionless |

*Subscripts*

| | |
|---|---|
| cr | = critical |
| $e$ | = excitation |
| fv | = free vibration |
| $i$ | = bending mode number |
| max | = maximum |
| $n$ | = PLF nose |
| no | = forwardmost point with zero modal value |
| sh | = shock |
| st | = static |
| $\infty$ | = freestream state |

Received March 4, 1997; revision received Jan. 28, 1998; accepted for publication Jan. 31, 1998. Copyright © 1998 by the American Institute of Aeronautics and Astronautics, Inc. All rights reserved.

*Engineering Specialist, Structural Dynamics Department, P.O. Box 92957-M4/909. Senior Member AIAA.

†Senior Engineering Specialist, Fluid Mechanics Department, P.O. Box 92957-M4/967.

‡Engineering Specialist, Vehicle Concepts Department, P.O. Box 92957-M4/919.

## Introduction

REFERENCE 1 presented a new closed-form solution for estimating the effects of launch vehicle aeroelastic coupling based upon a direct analysis of the system response to the input force variation. In the classical theory, the aeroelastic coupling is analyzed with respect to a prima facie threshold amplitude, below which the system response is perceived to diverge[2,3] due to the undamping effect of the input force variation. However, Ref. 1 showed that the force–response coupling relationship always yields a bounded response for structurally damped systems and that this amplitude cannot be arbitrarily varied to create a divergent condition as done in the classical theory. Reference 1 also observed that the amplification factor corresponding to the so-called stability criterion is consistent with an approximate analytic expression derived in Ref. 1, namely, Eq. (44), if the dynamic time lag implicit in the classical theory is explicitly defined. The limit cycle amplitude is roughly linear with respect to the time lag, and its definition is thus crucial in the prediction of launch vehicle loads from aeroelastic coupling. These loads must be realistically predicted to ensure flight readiness, and their overestimation can have highly undesirable programmatic impacts, including structural redesign and launch delays due to restrictions on the allowable winds. Flight data for the Titan IV launch vehicle (Fig. 1) have exhibited alternating flow. This work begins with a discussion of these data and the historical alternating flow wind-tunnel data. Aeroelastic coupling is then analyzed for a launch vehicle mission to illustrate the application of the present theory and to make comparisons with the classical theory.

## Wind-Tunnel and Titan IV Flight Data

Reference 4 demonstrated that for transonic Mach numbers the flow near the cone–cylinder junction (CCJ) of launch vehicle payload fairings (PLFs) can exist in one of two states. These wind-tunnel data indicated that, for freestream Mach numbers $M_\infty$ less than 0.89, the flow was separated at the CCJ, as shown in the center of Fig. 2a, and that for $M_\infty$ greater than 0.89, the corresponding flow was attached at the CCJ as seen in Fig. 2b. Further experimental investigations indicated that, for $M_\infty$ near 0.89, the flow became unstable and oscillated between the two states.[5] The data of Ref. 4 also showed that, for freestream Mach numbers slightly less than 0.89, the nominally separated flow at the CCJ on both sides of the pitch plane changes to attached flow on the windward side when the angle of attack exceeds a critical value. This is shown schematically in Fig. 2a, where the bending rotation angle is the effective angle of attack. For freestream Mach numbers just above 0.89, the data indicated that the nominally attached flow at the CCJ changes to separated flow on the leeward side when the angle of attack exceeds a critical value, as shown in Fig. 2b. The present theory defines the

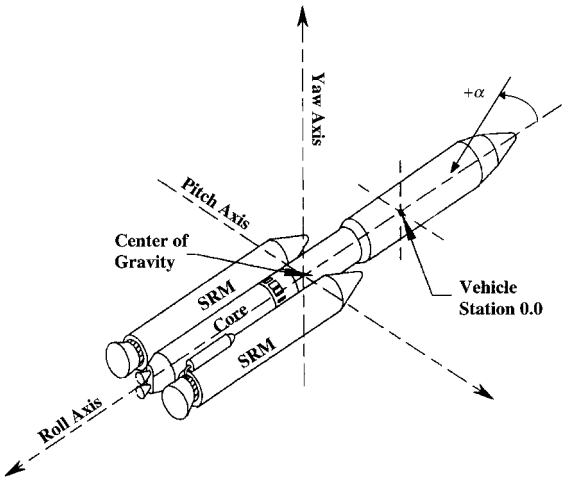


**Fig. 1 Coordinate system for Titan IV launch vehicle.**

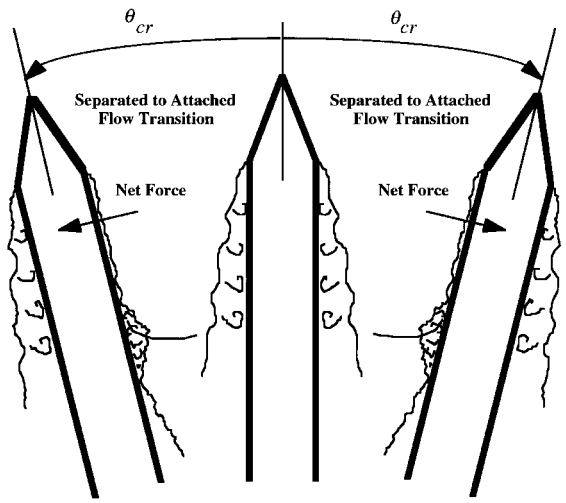


**a) $M_\infty < 0.89$ (windward-side transitions)**

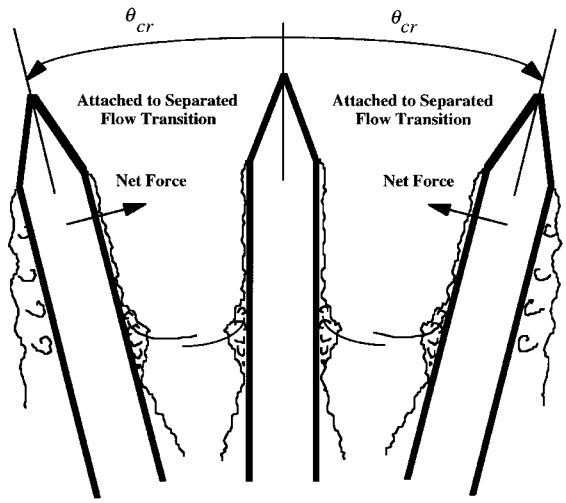


**b) $M_\infty > 0.89$ (leeward-side transitions)**

**Fig. 2 Wind-tunnel flow state changes.**

aeroelastic coupling in terms of the critical rotation angle $\theta_{cr}$, as shown in Fig. 3 of Ref. 1.

The locations of pressure transducers near the CCJ on the PLF, for a particular mission of the Titan IV, allowed the existence of alternating flow states to be detected during transonic flight. Figure 3 indicates at least four occurrences of alternating flow observed during this flight. The measured static pressures at two axial locations near the CCJ as a function of freestream Mach number are shown. In Fig. 3a, the data measured 5 in. aft of the PLF CCJ exhibit alternating flow between the nominal separated flow state and the alternate

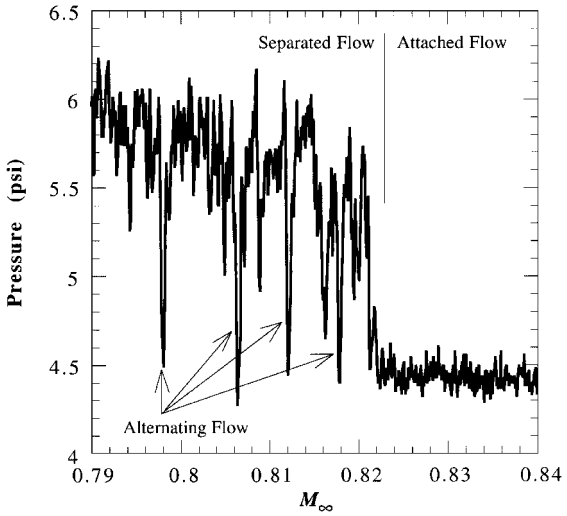


**a) Transducer located 5 in. aft of PLF CCJ**

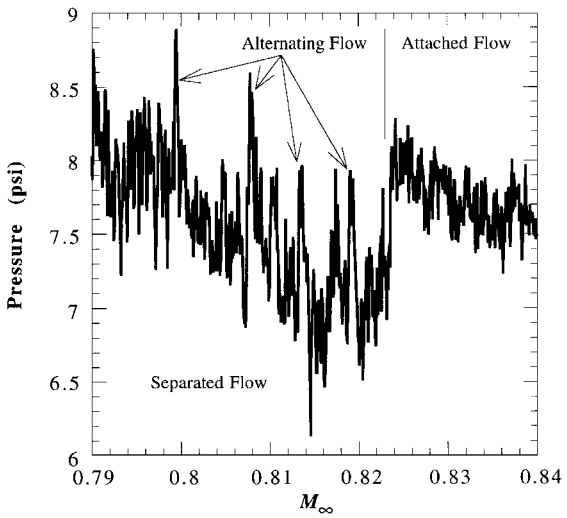


**b) Transducer located 50 in. aft of PLF CCJ**

**Fig. 3 Titan IV flight pressure measurements.**

attached flow state. When the change occurs, the static pressure decreases in a manner consistent with the pressure coefficient data at 5 in. shown in Fig. 2 of Ref. 1. In Fig. 3b, the data measured 50 in. aft of the PLF CCJ again show alternating flow between the nominal separated flow state and the alternate attached flow. The oscillations are highly correlated in Mach number with those at the 5-in. station, and in this case the static pressure increases, which again is consistent with the pressure coefficient data for $x = 50$ in. in Fig. 2 of Ref. 1. The flight data in this respect are thus consistent with the oscillating flow states described in Ref. 5. Oscillations like these were not observed in other Titan IV missions with these pressure transducers.

Figure 4 shows the angle of attack–Mach number zone of (wind-tunnel) alternating flow defined in Ref. 5 for a 20-deg PLF cone angle. The Mach number range corresponding to alternating flow for the Titan IV mission falls to the left of this elliptical zone. The oscillations, nevertheless, are consistent with those shown in Fig. 2a and are thus consistent with the wind-tunnel data. Also included for comparison in Fig. 4 are angle-of-attack histories for 15 flights of the Titan IV determined using a trajectory simulation with the prelaunch wind sounding. The angle of attack experienced by the Titan IV during transonic flight is generally smaller than ±1 deg because of the vehicle steering program and onboard control system.[6] The time history for the mission known to have experienced oscillating flow on the windward side of the pitch plane is accentuated.

The net force acting on the PLF due to the condition of asymmetric flow states may be in phase with the structural displacement, as shown in Fig. 2a, or out of phase, as shown in Fig. 2b. The phasing

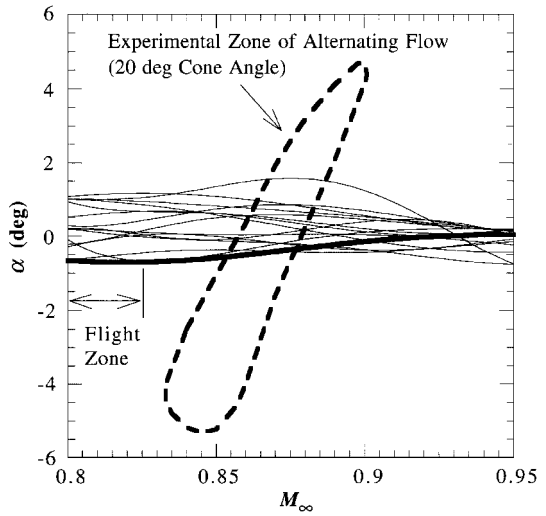


**Fig. 4 Titan IV flight trajectories and experimental zone of alternating flow.**

is not determined by the Mach number being greater than or less than 0.89 but rather by the pressure coefficient distributions for the separated and attached flow states. The forces acting on a Titan IV PLF were calculated in Ref. 1 using pressure coefficients from wind-tunnel data exhibiting the separated and attached flow states at the CCJ of the PLF. If the flow on the Titan IV PLF is asymmetric, as shown in Fig. 2, the net force resultant equals 4400 lbf acting in the direction of the structural displacement, regardless of whether the asymmetry occurs for freestream Mach numbers less than or greater than 0.89. Because the net force is in the direction of the displacement, it is always in phase with the displacement if the flow states become asymmetric. Reference 1 proved using energy principles that the net force must be out of phase with the displacement for limit cycles to occur. The Titan IV launch vehicle, therefore, is not susceptible to self-sustained aeroelastic coupling.

## Analysis with Coupled Launch Vehicle Model

The theory developed in Ref. 1 was applied in an analysis of a Titan IV mission. Force magnitudes corresponding to the pressure profiles in Fig. 2 of Ref. 1 were used, but the signs were changed so that aeroelastic coupling would be induced; this occurs because the sign change has the effect of making the net force out of phase with the launch vehicle response. The analytic forces, therefore, are synthetic, and the corresponding responses could not be exhibited by the Titan IV during flight. The heuristic analysis was conducted with a complete transonic dynamic model to assess the magnitudes of launch vehicle limit cycle loads and to verify that aeroelastic coupling can be analyzed as a single-degree-of-freedom (SDOF) system.

### Analysis Approach for Titan IV Mission

The PLF for the launch vehicle analyzed is 76 ft long. A transonic dynamic model with coupled system modes up to 100 Hz was used. The system mass during transonic flight is not constant because the solid rocket motor propellant is being consumed, but the equations of motion are taken to be stationary, an acceptable assumption for Titan IV airloads analyses less than 10 s in duration. The alternating flow forces were assumed to couple with the fundamental bending mode, which induces the largest launch vehicle loads. Figure 5 shows this mode normalized with respect to its maximum value.

The force amplitudes and application points were held constant during the analysis; values for Mach 0.8 were used because they generate more severe responses than those for higher transonic Mach numbers and because alternating flow was observed in Titan IV flight data around this time point. The locations of the force resultants, $F_1$ and $F_2$, shown in Fig. 2 of Ref. 1 do not coincide with node points of the PLF dynamic model. Each force was translated to the nearest node and was adjusted to ensure an equivalent pitch force and moment. The duration of the excitation was taken to be approximately 3 s, the time that it takes the Titan IV to fly through the region $M_\infty = 0.8$–$0.9$. Free vibration was induced by stopping the forces at the end of a half-cycle. The critical nose bending rotation for initiating a change of flow state was assumed to equal the value corresponding to $t_a = 0$ in Fig. 3 of Ref. 1, i.e., very nearly 0 deg.

**Table 1 Transient response analysis parameters**

| Property | Time lag, ms 7 | Time lag, ms 14 | Ref. 1, Eq. |
|---|---|---|---|
| $\Delta t/\zeta T_i$ | 1.3 | 2.6 | —— |
| $T_e/T_i$ | 0.83 | 0.90 | (40) |
| $T_e$, s | 0.62 | 0.67 | —— |
| $f_e$, Hz | 1.6 | 1.5 | —— |
| $3f_e$, Hz | 4.9 | 4.5 | —— |
| $q_{st}$, in. | 5.7 | 5.7 | (11) |
| $\theta_{st}$, deg | 0.044 | 0.044 | —— |
| $z_{cr}$ | 0.11 | 0.37 | (23) |
| $\theta_{cr}$, deg | 0.005 | 0.016 | —— |
| AF | 2.8 | 5.4 | (20) |
| $\theta_{max}$, deg | 0.12 | 0.24 | —— |
| $AF_{fv}$ | 3.6 | 6.2 | (30) |
| $\theta_{fv}$, deg | 0.16 | 0.27 | —— |

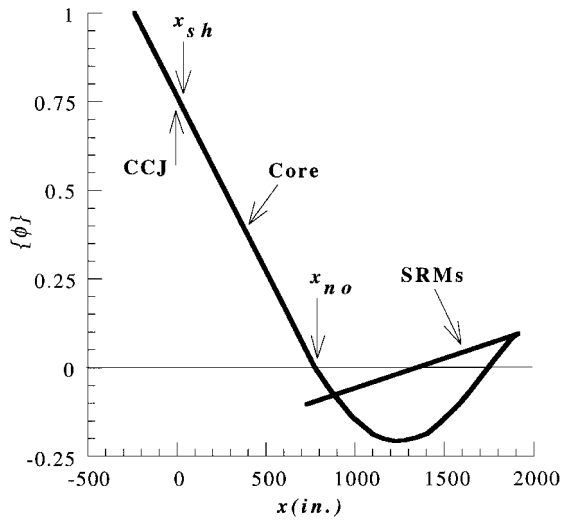


**Fig. 5 Fundamental bending mode shape for Titan IV mission with 76-ft PLF.**

For this study, the aerodynamic time lag was based on the Titan IV flight data. The flow transitions observed in the pressure measurements of Fig. 3 indicate that the time required for each of the four disturbances to travel from the forward to the aft transducer fell in the range 5–7 ms. Reference 3 defines a time lag as the distance between the centroids for the separated and attached pressure profiles divided by an estimated convection velocity but then does not use this time lag in the analysis of the current problem. This approximation yields 6 ms for the profiles shown in Fig. 2 of Ref. 1. The distance between the flight transducers equaled 45 in., somewhat larger than the difference in the centroids. Titan IV flight data, therefore, suggest that 7 ms is a conservative estimate of the aerodynamic time lag. Additional results were generated by arbitrarily doubling this value.

A transient response computer program solved Eq. (1) of Ref. 1 given the Titan IV modal parameters and the semiempirical force time histories. An initial generalized displacement for the fundamental bending mode was specified. Its value corresponded to the amplification factor for the limit cycle state based on the single mode representation. All other initial displacements and velocities were set to zero. The force–response relationship for aeroelastic coupling was not explicitly satisfied. However, if the force variation and initial condition are correctly predicted, the computed response is periodic and implicitly satisfies this relationship. The fundamental bending mode was identified by examining the modal kinetic energy for the coupled system. The frequency and damping of the selected mode equal 1.344 Hz and 0.72%, respectively. Parameters corresponding to the input force variation and initial condition are listed in Table 1

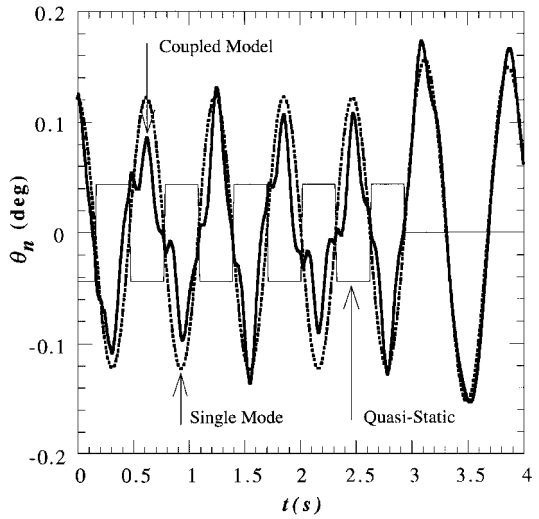


a) $\Delta t$ = 7 ms

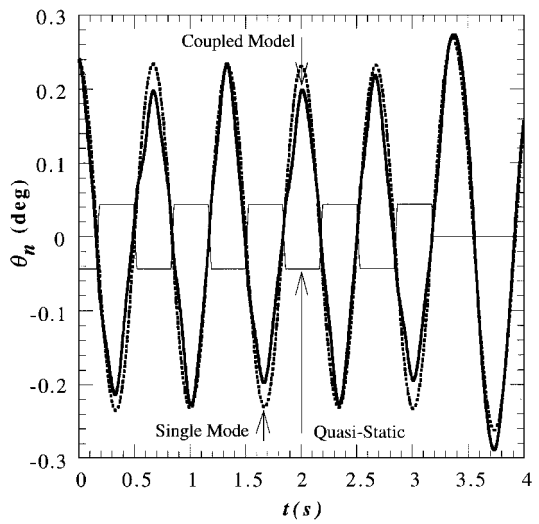


b) $\Delta t$ = 14 ms

**Fig. 6 Comparison of single mode and coupled model responses.**

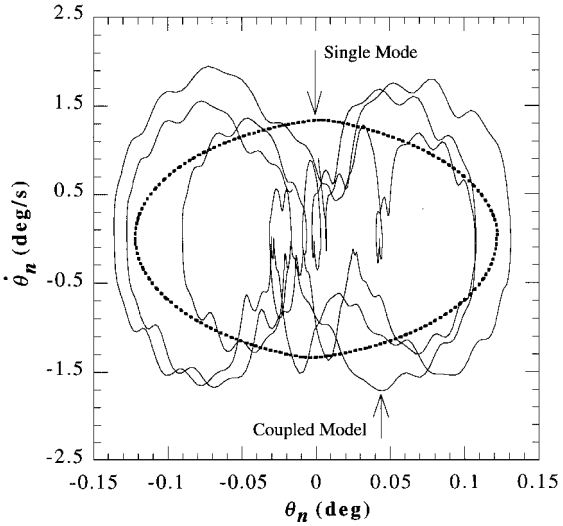


**Fig. 7 Phase plane diagram of single mode and coupled model responses ($\Delta t$ = 7 ms).**

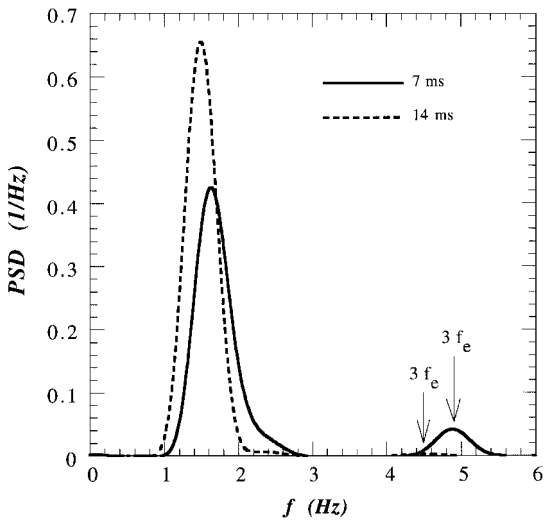


**Fig. 8 Power spectral density of coupled model responses.**

with the equation numbers of the analytic expressions in Ref. 1 used to predict them.

#### Applicability of Single Mode Representation

Figures 6a and 6b show output from the computer transient response program for $\Delta t = 7$ and 14 ms, respectively. The time histories of the PLF tip rotation were recovered using the computed generalized responses for the single bending mode and for the entire mode set. The quasistatic time histories shown correspond to the input force variation. In both plots, the single mode response is periodic, which confirms that the limit cycle state for the SDOF system was accurately predicted by the parameters in Table 1. Further evidence of the periodicity is provided in Fig. 7, in which a phase plane diagram of the forced parts of the computed responses is shown for the 7-ms time lag case. The coupled model response oscillates raggedly about the single mode response in Fig. 7, and only the last three cycles are plotted for clarity. Figure 6b shows that the coupled model response history is in better agreement with the single mode response for the 14-ms time lag case. An explanation for this difference follows.

Equation (41) of Ref. 1 indicates that the frequencies of the terms in the Fourier series expansion of the force variation equal $n/T_e$. The higher-order Fourier components of the alternating flow forces, therefore, may excite system modes other than the bending mode with which the force variation was intended to couple. The amplitudes of the Fourier terms decrease as $n$ increases, such that the degree of this extraneous excitation generally diminishes as the frequency increases. Figure 8 shows plots of power spectral density (PSD) computed from the forced parts of the coupled model responses for the two time lag cases. The time histories were normalized with respect to their initial value and padded with zeros to smooth the PSD curves. Table 1 indicates that the second Fourier component ($n = 3$) has a frequency equal to 4.9 and 4.5 Hz for time lags defined by 7 and 14 ms, respectively. The frequency of the third bending mode of the Titan IV dynamic model equals 5.1 Hz. The coupled model response in Fig. 6a, therefore, differs from the single mode response primarily because of unintended excitation of the third bending mode. The agreement between these two curves improves in Fig. 6b because the second Fourier term shifts away from the third bending mode. It can be concluded that the accuracy of the single mode representation depends on the excitation period $T_e$ and the frequency content of the system dynamic model.

#### Aeroelastic Load Comparison with Other Airloads Components

In the single mode representation, the maximum launch vehicle loads from aeroelastic coupling are defined by

$$\{L\} = \mathrm{AF} q_{\mathrm{st}} [\mathrm{LTM}]\{\phi\} \tag{1}$$

Figure 9 shows the pitch moment as a function of vehicle station (Fig. 1) for the Titan IV mission analyzed in the previous section. The mean components of the dynamic transonic airloads are compared with the mean aeroelastic coupling loads. Static aeroelastic loads corresponding to a 1-deg angle of attack are included for comparison; the actual static aeroelastic loads for the mission are computed

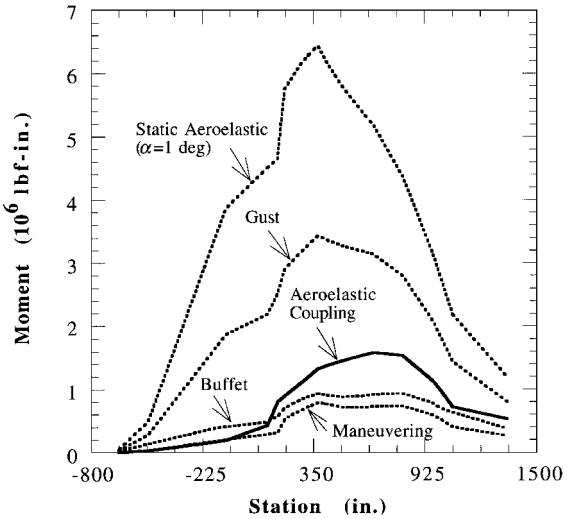


**Fig. 9 Mean pitch bending moment for dynamic transonic airloads components.**

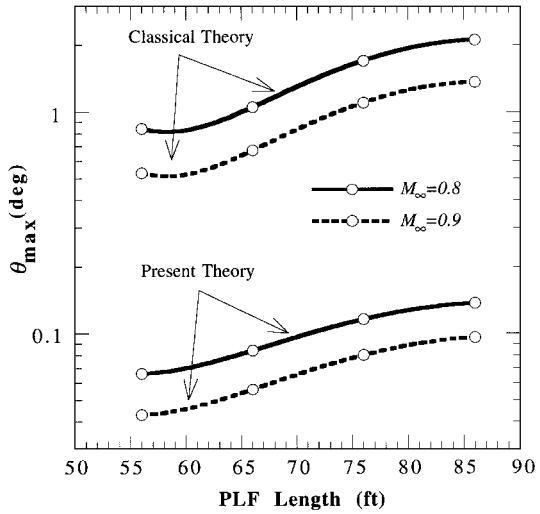


**Fig. 10 Limit cycle amplitudes for aeroelastic coupling with fundamental bending mode.**

on the day of launch based on wind sounding.[6,7] The mean aeroelastic coupling loads shown correspond to alternating flow forces with a 7-ms time lag and equal one-third of the total loads from Eq. (1). The latter is generally consistent with the definition of mean loads for the buffet and gust events; the remaining two-thirds of the total loads are treated as dispersions. Loads similar to those shown in Fig. 9 exist in the yaw plane. The total loads are computed using a combination equation with the mean and dispersed load components in both planes.[7]

It bears repeating that the signs of the Titan IV flow separation resultants were perforce reversed to induce aeroelastic coupling and that the effect of the control system was neglected. The results, nevertheless, provide a heuristic measure of aeroelastic coupling loads relative to the other transonic load components. For the mission considered, the aeroelastic coupling loads are generally larger than those for buffet and maneuvering but are smaller than those for gust. It can be concluded that, if the sum of the alternating flow forces is out of phase with the bending mode displacement response, the corresponding aeroelastic loads should be assessed and that aeroelastic coupling can have a significant effect on the total transonic airloads that a launch vehicle must withstand.

## Comparisons with Classical Theory

### Effect of Payload Fairing Length

The effect of the length of the payload fairing on the limit cycle amplitude was assessed using both the present and the classical theories. Modal data for Titan IV missions with PLF lengths equal to 56, 66, 76, and 86 ft were used. Results, in terms of the maximum nose deflection angle, for coupling with the fundamental bending mode are compared in Fig. 10 with the so-called stability criterion results from the classical theory. A 7-ms aerodynamic time lag was used in the implementation of the present theory. Limit cycle amplitudes based on Titan IV pressure profiles at $M_\infty = 0.8$ and 0.9 are shown.

The present and classical theories yield similar trends. The limit cycle amplitude increases monotonically with payload fairing length and is less for the higher transonic Mach number. The stability criterion results, however, are 12–16 times larger than the limit cycle amplitudes from the present theory, depending on the payload fairing length. The aeroelastic coupling loads shown in Fig. 9 are commensurate; in the middle of the launch vehicle core, the classical theory yields a much larger mean pitch moment, equal to $23 \times 10^6$ lbf-in. for this mission. Predicted moments of this magnitude would, at the very least, cause severe restrictions on the allowable day-of-launch winds and, consequently, launch availablility.

### Definition of Generalized Time Lag

The differences between the maximum nose deflection angles and pitch moments predicted by the present and the classical theories are caused primarily by the magnitude of the time lag defined by the two approaches. This is because the amplification factor is nearly linearly proportional to the time lag. In the present theory, this parameter is the aerodynamic time lag and is an input variable. In the classical theory, the dynamic time lag is defined implicitly by the analysis assumption that the dynamic motion affects the critical flow transition angle and thereby introduces a dynamic hysteresis. It can be shown that the amplification factor corresponding to the so-called stability criterion is the same as that given by the present theory when a harmonic approximation is used, i.e.,

$$\mathrm{AF} = 2(\Delta t/\zeta T_i) \tag{2}$$

and that, for the classical theory, the dynamic time lag equals

$$\Delta t_d \cong \frac{x_{\mathrm{no}} - x_{\mathrm{sh}}}{U_\infty} + \frac{0.9D}{U_{\mathrm{sh}}} \tag{3}$$

The distances $x_{\mathrm{no}}$ and $x_{\mathrm{sh}}$ are illustrated in Fig. 5. For the Titan IV at Mach 0.8, Eq. (3) yields values of $\Delta t_d$ between 90 and 120 ms, depending on the PLF length. These values are more than an order of magnitude larger than the aerodynamic time lag based on the distance between pressure profile centroids and a convection velocity, and they increase the amplification factor proportionately. The factors that could contribute to a generalized time lag can thus be differentiated as follows:

$$\Delta t = \Delta t_d + \Delta t_a \tag{4}$$

in which the first term is the dynamic time lag and the last term is the aerodynamic time lag. Summarizing concisely, in the classical theory the aerodynamic time lag is assumed to be zero, whereas in the present theory it represents the sole term.

The dynamic time lag consists of crossflow and adverse pressure gradient contributions that are estimated implicitly in the classical theory by the respective terms in Eq. (3). There appears to be no test data to support the implicit time lag used in the classical theory. Equation (3) is based on analysis assumptions and the governing equations for the fluid. Wind-tunnel test data exhibiting alternating flow do not provide estimates of the crossflow effect. These data were acquired for a fixed test article. Measurements were taken for a given angle of attack, and then the test setup was changed. To assess the crossflow effect, the test article would have to move laterally with respect to the mean flow velocity. The present work concludes that a limit cycle can be induced by aerodynamic or dynamic time lags and concisely and dramatically illustrates the effect of the very large dynamic time lags implied by the classical theory. The importance of obtaining an accurate estimate of the generalized time lag is readily apparent.

## Conclusions

The current work consolidates the classical and present theory and shows that considerably larger responses and loads result if the dynamic time lag defined implicitly by the classical theory is real. The magnitude of aeroelastic coupling loads can be very significant compared with those for other transonic airloads events, hinging on the magnitude of a generalized time lag defined in the present work. The magnitude of the generalized time lag depends on the mechanisms that define coupling. Further work is needed to characterize the nature of the coupling mechanisms because of their large impact on the time lag. The assumption of a single bending mode response for aeroelastic coupling is acceptable provided that the higher-order Fourier component frequencies of the force are not very close to other system modes in the plane of the coupling. The Titan IV is not susceptible to self-sustained aeroelastic coupling because the net force acting on the vehicle, when asymmetric flow states exist on the payload fairing, is in phase with the displacement.

## Acknowledgments

This work was supported by the U.S. Air Force Materiel Command, Space and Missile Systems Center, under Contract F04701-93-C-0094. The mode shapes and modal parameters used to compute the limit cycle amplitudes shown in Fig. 10 were provided by Lockheed Martin Corporation.

## References

[1]Dotson, K. W., Baker, R. L., and Sako, B. H., "Launch Vehicle Self-Sustained Oscillation from Aeroelastic Coupling Part 1: Theory," *Journal of Spacecraft and Rockets*, Vol. 35, No. 3, 1998, pp. 365–373.

[2]Ericsson, L. E., "Aeroelastic Instability Caused by Slender Payloads," *Journal of Spacecraft and Rockets*, Vol. 4, No. 1, 1967, pp. 65–73.

[3]Ericsson, L. E., and Reding, J. P., "Fluid Dynamics of Unsteady Separated Flow, Part I. Bodies of Revolution," *Progress in Aerospace Sciences*, Vol. 23, 1986, pp. 1–84.

[4]Robertson, J. E., and Chevalier, H. L., "Characteristics of Steady-State Pressures on the Cylindrical Portion of Cone-Cylinder Bodies at Transonic Speeds," Arnold Engineering Development Center, AEDC TDR-63-104, Tullahoma, TN, Aug. 1963.

[5]Chevalier, H. L., and Robertson, J. E., "Pressure Fluctuations Resulting from an Alternating Flow Separation and Attachment at Transonic Speeds," Arnold Engineering Development Center, AEDC TDR-63-204, Tullahoma, TN, Nov. 1963.

[6]Dotson, K. W., and Tiwari, S. B., "Formulation and Analysis of Launch Vehicle Maneuvering Loads," *Journal of Spacecraft and Rockets*, Vol. 33, No. 6, 1996, pp. 815–821.

[7]Macheske, V. M., Womack, J. M., and Binkley, J. F., "A Statistical Technique for Combining Launch Vehicle Atmospheric Flight Loads," AIAA Paper 93-0755, Jan. 1993.

R. B. Malla
*Associate Editor*